A Regenerative Controllable DC Load for an Electric Vehicle Test Station

M. Thorne and M. Kazerani, *Senior Member, IEEE*
Department of Electrical & Computer Engineering, University of Waterloo
Waterloo, Ontario, Canada
mthorne@engmail.uwaterloo.ca, mkazeran@ecemail.uwaterloo.ca

***Abstract*—Programmable DC loads presently available on the market lack power reversal capability, which is an essential feature required for testing various topologies and power management algorithms for electric vehicle powertrains. In this paper, a controllable DC load with regenerative capability is introduced and tested. It is shown through analysis and simulation that the proposed load can be controlled to emulate the drivetrain power requirements from the viewpoint of high-voltage DC bus, during any arbitrary drive-cycle consisting of periods of acceleration, cruising, deceleration and stopping. The proposed load has the potential of being incorporated in test stations for battery-electric and fuel cell-electric vehicles.**

***Index Terms*—Electric vehicle, Test Station, Programmable load, Regenerative Braking**

I. Introduction

In the world today, there is an outcry for more efficient and environmentally-friendly ways of producing and using energy. More efficient vehicles are a top priority. Part of the research concerning lower emissions and higher efficiency involves a battery-electric or fuel cell-electric drivetrain equipped with regenerative braking.

Regenerative braking is a novel concept commonly used in electric and hybrid electric vehicles to capture the kinetic energy stored in the rotating parts of the moving vehicle, when an attempt is made to stop the vehicle or reduce its speed. The energy captured is converted to electrical energy, and stored in a battery or ultracapacitor bank to be used later when the energy is needed, e.g., during acceleration, thus reducing running costs [1] [2]. A practical study reported in [1] proves that incorporating a regenerative braking system in a city bus, featuring frequent stops and short acceleration periods, would yield a potential savings of close to 60%.

In order to perform experimental study on battery-electric and hybrid fuel cell vehicles in the setting of a lab, a scaled-down or a full-scale test bed is normally used. In such test stations, a controllable DC load can effectively emulate the power required by the drivetrain at the interface with the high-voltage DC bus. Off-the-shelf controllable DC loads lack regenerative capability. They can be used for simulating a passive DC load profile as well as for testing the capabilities of different DC sources such as switch-mode power supplies, fuel cells, solar arrays, and batteries. Such loads are costly and their design details are not available to customers. Also, the capabilities of these devices are limited. The controllable DC load introduced in [3] features simplicity, speed, cost effectiveness, and versatility, but can support only one direction of power flow. Therefore, it cannot be used to emulate a vehicular load in a test bed where regenerative braking has to be studied. To allow full study of regenerative braking operation in an electric vehicle, the controllable load used must accommodate bidirectional power flow.

This paper outlines the development process of a regenerative controllable DC load based on a bidirectional DC/DC converter. This system can simulate the combination of motor controller, electric motor and the forces exerted on the vehicle due to the friction between the tires and the road, air resistance, and moving uphill or downhill, as seen from the high-voltage DC bus. In the following, first an appropriate topology for the required bidirectional DC/DC converter is selected. Then, the design of the load's power and control circuits is presented. Finally, simulation results are presented to verify the capabilities claimed for the proposed controllable DC load.

II. Selection of Bi-Directional DC/DC Converter Topology

In this section, a few topologies for bidirectional DC/DC converter are investigated to select the most appropriate configuration for the controllable DC load application.

A. Two-Stage and Three-Stage Bidirectional Converters

A two-stage and a three-stage bidirectional DC/DC converters have been proposed in [4] for connecting batteries and ultracapacitors to the DC bus of a fuel cell-powered system. Battery and ultracapacitor are used in fuel cell systems for energy storage to enable the system to respond quickly to fast load changes that cannot be followed by the fuel cell, and make up for the delays involved in fuel cell cold starts.

The circuit diagram of the two-stage bidirectional DC/DC converter topology, also known as bidirectional buck-boost converter, is shown in Fig. 1(a). The control strategy is very straightforward. To control the power flow from the high-voltage side to the low-voltage side, the converter operates in the buck mode, where the switch Q_1 is turned on and off according to a PWM pattern to realize the desired amount of power transferred, and Q_2 is left in the off position while its anti-parallel diode participates in the operation. If it is necessary to reverse the direction of power flow, the converter is operated in the boost mode, where the switch Q_2 is turned on and off under PWM control to make the power transfer follow the corresponding reference signal, and Q_1 is left in the off position while its anti-parallel diode participates in the operation.

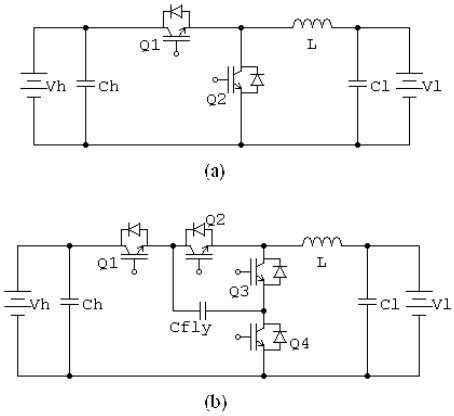

Fig. 1 Bidirectional DC/DC converter topologies [4]: (a) Two-stage topology; (b) Three-stage topology.

The disadvantages of the design shown in Fig. 1(a) are in high voltage stress on the switches and large components required when the input voltage is large, making the design bulky and expensive.

To overcome the drawbacks of the two-stage bidirectional DC/DC converter of Fig. 1(a), the three-stage topology shown in Fig. 1(b) has been proposed in [4]. Adding another stage, with two more switches and a capacitor, complicates both power circuit and control system, and makes the design more costly. The advantages of the new design are in lower voltage stress on the switches and slightly smaller components.

B. Isolated Bidirectional DC/DC converter Topologies

The isolated bidirectional DC/DC converter topology proposed in [5] and shown in Fig. 2, has a higher degree of complexity compared with those proposed in [4]. The converter employs a full-bridge DC-DC converter (also known as H-bridge) on the low-voltage side of the isolation transformer and a half-bridge converter on the high-voltage side. The switch S_c is an auxiliary switch that controls the clamp capacitor. Advantages of this topology include zero-voltage switching operation for all switches, constant clamping voltage across all switches, simple gate driver implementation, no voltage overshoot, no snubbing requirement, and electric isolation.

Although this is an interesting design, the goal is to keep the bidirectional DC/DC converter as simple and inexpensive as possible. This design uses seven switches and a transformer, complicating both power and control circuits, and making the design bulky and costly.

The isolated bidirectional converter topology shown in Fig. 3 has been proposed for interfacing energy storage devices with a DC bus [6]. It is composed of two H-bridges on the two sides of an isolation transformer. The advantages of this design are capability of voltage level adjustment and isolation. The disadvantages are in the use of a high-frequency isolation transformer and a large number of switches, as well as limitation in the permissible DC voltage range based on power loss and peak current considerations. It can be seen that, for both designs shown in Figs. 2 and 3, the advantages do not outweigh the complexity.

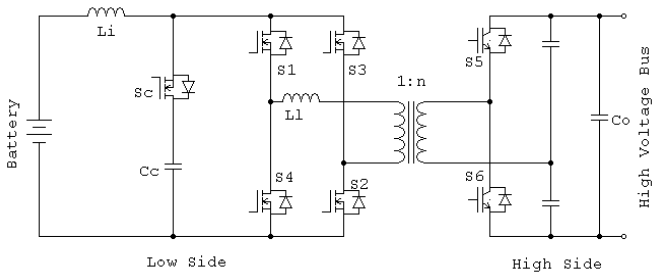

Fig. 2 Isolated bidirectional DC/DC converter [5]

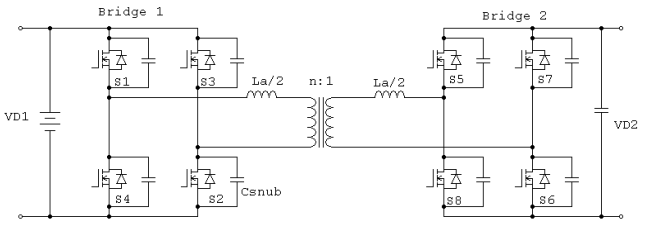

Fig. 3 Isolated bidirectional DC/DC converter [6]

C. Full-Bridge DC/DC Converter

The full-bridge DC-DC converter shown in Fig. 4 [7] is bidirectional. The advantages of this converter topology are its simplicity of design and control, and lower number of switches compared with other H-bridge-derived topologies. The disadvantages are in the use of higher number of switches with respect to the bidirectional buck-boost topology and the fact that two low-pass L-C filters, one on each side, are required, resulting in a comparatively higher cost and complexity.

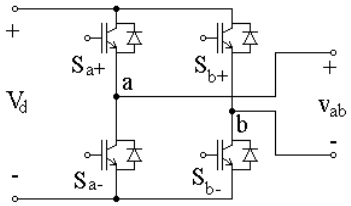

Fig. 4 H-bridge DC/DC converter [7]

D. Choosing a Topology

After careful comparison of different possible bidirectional DC-DC converter topologies from the viewpoints of simplicity of design, number of components used, cost, ease of control and performance, the bidirectional buck-boost converter topology emerges as the superior design for the regenerative controllable DC load.

III. PROPOSED REGENERATIVE CONTROLLABLE DC LOAD

A. Power Circuit

The circuit diagram of the proposed regenerative controllable DC load, based on the bidirectional buck-boost converter topology, is shown in Fig. 5. S_1 and S_2 are the main switches of the bidirectional buck-boost converter. When the direction of power flow is from the high-voltage (source) side to the low-voltage (battery) side, the converter operates as a buck converter, as shown in Fig. 6(a). When power flows in

the opposite direction, the converter operates as a boost converter, as shown in Fig. 6(b). In each mode of operation, one switch and the anti-parallel diode across the other switch are operational. At the low-voltage side of the converter, a resistor and a battery are connected in parallel. The resistor-battery combination represents the power consumed by the load (power flow from the high-voltage side to the low-voltage side) and the energy stored in the load to be returned to the source (power flow from low-voltage side to the high-voltage side). When the system of Fig. 5 represents a vehicular load in an electric or hybrid fuel cell vehicle test bed, the power flow from the high-voltage side to the low-voltage side represents motoring mode of the electric machine coupled with the wheels, whereas power flow from low-voltage side to the high-voltage side indicates regenerative braking.

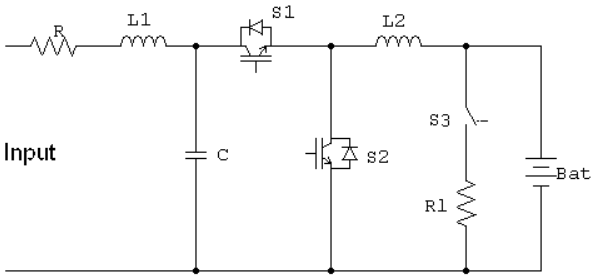

Fig. 5 Proposed regenerative controllable DC load

Buck mode is considered the normal operational mode and is used when the vehicle is requesting power from the high-voltage DC bus for propulsion (positive direction of power flow). This power is used to recharge the battery until the state-of-charge of the battery exceeds a pre-set level. This ensures that the battery will be able to provide the power equivalent to regenerative braking power when required. When the battery charge exceeds a pre-determined level, the power will be dissipated in R_l by turning the switch S_3 on.

Boost mode is the mode that simulates the regenerative braking (negative direction of power flow). In this case, R_l is disconnected by turning the switch S_3 off, and the battery discharges as power flows out of its terminals towards the high-voltage side. The energy supplied by the battery simulates the electric energy recovered via regenerative braking. In an actual electric vehicle, or an electric vehicle test station, the regenerative braking energy is normally stored in storage batteries or ultra-capacitors on the high-voltage DC bus for future acceleration and high-power-demand periods in the drive cycle.

The purpose of the resistor R connected in series at the input terminals of the controllable load is to convert the difference between the load input voltage and the voltage reflected on the source-side of the bidirectional buck-boost converter into a current. The direction of this current depends on the sign of the potential difference across the resistor R (positive in the buck mode and negative in the boost mode), and represents the direction of power flow. This resistor is very small and results in a very small power loss. Note that the equivalent series resistance of the input filter inductor may be large enough to serve the purpose of the resistor R.

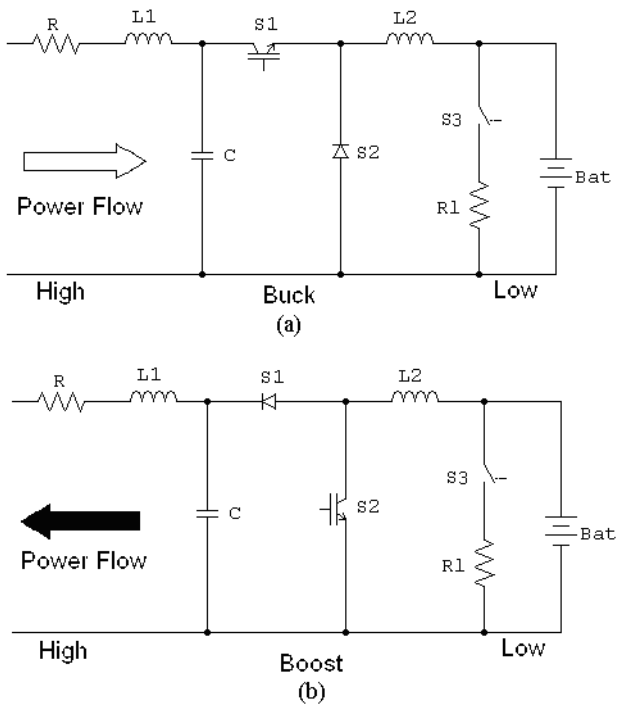

Fig. 6 Operational modes of the proposed regenerative controllable DC load: (a) Mode 1: Buck – load drawing power from the source, (b) Mode 2: Boost – load supplying power to the source

The load should be sized based on the full power of the simulated vehicle. In this paper, the maximum power of the load was chosen to be 3kW. The maximum input voltage of the load and the battery voltage were taken as 100V and 60 V, DC, respectively. The rather high value of the battery voltage serves to keep the current corresponding to maximum power flow below safe limits. A detailed battery model is used to allow for observing the operation of the battery and monitoring its state-of-charge (SOC), incorporating actual limits on the amount of power it can provide for a given length of time, and also making the simulations more realistic. The battery model used is shown in Fig. 7 [8].

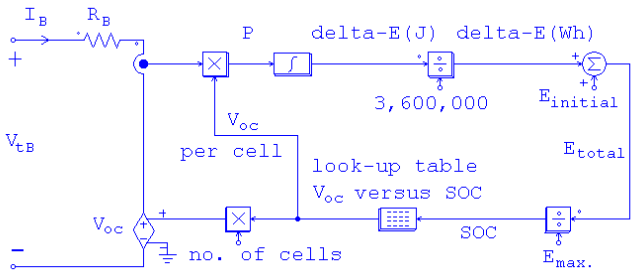

Fig. 7 Battery model used in simulations [8]

The look up table in Fig. 7 provides the open circuit voltage of the battery in terms of its state-of-charge. The battery that was used for this model was EnerSys Genesis EP, Pure-lead 12V battery, and the information for the lookup table and the capacity (in kWh) was found on the specification sheet provided on the EnerSys website [9]. To achieve 60V at the low-voltage side, five 12-V batteries were connected in series.

Based on the maximum voltage of the low-voltage side of the converter, the required value of R_l, that can dissipate the maximum power absorbed by the load when the battery is almost fully charged, can be easily calculated as follows.

$$P_{\max} = \frac{V_{battery}^2}{R_l} \rightarrow R_l = \frac{V_{battery}^2}{P_{\max}} = \frac{60V^2}{3000W} = 1.2\Omega \quad (1)$$

By Ohm's Law, the maximum current drawn by R_l can be calculated as

$$I = \frac{V_{battery}}{R_l} = \frac{60V}{1.2\Omega} = 50A \quad (2)$$

In (1) and (2), $V_{battery}$ is the battery terminal voltage, which is assumed to be equal to 60V. This is a reasonable assumption since the resistor R_l is switched in when the battery's state-of-charge is high, and battery voltage does not deviate considerably from 60V under such conditions. R_l will always draw 50A when S_3 is closed. If the load is not operating at maximum power, and thus, the current reaching the battery-R_l combination is less than 50A, the remaining current will be provided by the battery. When the charge of the battery drops below the set point, S_3 will open and the battery will resume charging until it exceeds the set point again, in which case the cycle repeats. This will be the case until switch S_3 is opened upon reversal of power flow direction.

B. Control Circuit

The objective is to control the power at the input terminals of the controllable DC load according to a reference. The reference signal for the power at the terminals of the load is derived in the following way. First, a drive cycle and a vehicle are chosen. The Environmental Protection Agency (EPA) provides several drive cycles on their website, which are used for testing emissions on new vehicles manufactured by automotive companies that sell vehicles in the United States [10]. In this study, the urban drive cycle (Fig. 8) was used for its frequent stops and accelerations.

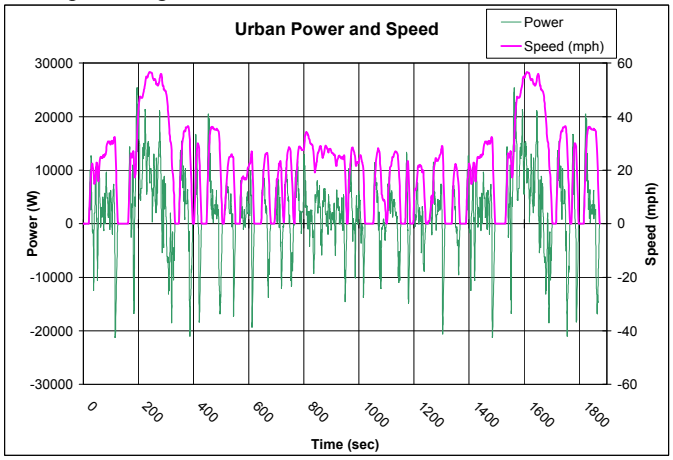

Fig. 8 Speed and power of Urban Drive Cycle

Once an acceptable drive cycle is selected, an algorithm needs to be developed to convert the speed-versus-time data to power-versus-time information based on the selected vehicle. In order to do this, the power required by the vehicle over the drive cycle has to be determined, taking the power losses due to drag and the friction between the tires and the road into account. The derivation of the algorithm is outlined by (3)-(6) [11]. First, the gross power is formulated as:

$$P_{gross} = F \times v = m \times a \times v \quad (3)$$

Then, the powers associated with friction and drag are given as:

$$P_{friction} = F_{friction} \times v = \mu \times F_N \times v = \mu \times mg \times v \quad (4)$$

and

$$P_{drag} = F_{drag} \times v = (\frac{1}{2} C \rho A v^2) \times v = \frac{1}{2} C \rho A v^3 \quad (5)$$

The net required power will therefore be:

$$P_{net} = P_{drag} + P_{friction} + P_{gross} = \frac{1}{2} C \rho A v^3 + \mu mgv + mav \quad (6)$$

In (3)-(6), F stands for force, P for power, m for mass, A for cross-sectional area, C for drag coefficient, μ for coefficient of friction, g for gravitational acceleration, v, for speed, a for acceleration and ρ for air density. In order to determine the load's input power reference signal, the parameters provided by the vehicle manufacturer are plugged in (6) to calculate the power required to take the vehicle through the drive cycle. In (6), velocity, v, is determined by the drive cycle and acceleration, a, is calculated from the rate of change with respect to time of velocity from one data point to the next. The calculated power has to be scaled down so that the maximum required powers for propulsion and regenerative braking fall below the rated power of the load. The vehicle used in this study is a typical North American sedan, with the parameters given in the Appendix. The range of required power over the drive cycle was found to be -21,227.6 - 25,375.86 W. The power was scaled down by a factor of 0.1 to fall within the [-3, 3]-kW range of power supported by the load designed in this work. Fig. 8 shows the calculated power versus time together with the corresponding EPA urban drive cycle.

In the course of controller design and simulation of the controllable load, it was found to be more effective to control the power on the low-voltage side, i.e., at the terminals of the battery-R_l (B-R_l) combination, rather than the power at the input terminals of the load. To derive the reference signal for the power on the low-voltage side from the reference signal for the power at the load input terminals, the power loss due to the current flowing in the resistor R at the load input terminals has to be taken into consideration. The calculations involved in finding the expected power loss in R and the current reference signal on the low-voltage side at the terminals of B-R_l combination are given by (7).

$$P_{R,loss} = I_R^2 R = \left(\frac{P_{load,ref.}}{V_{in,load}} \right)^2 \times R$$
$$I_{B-R_l,ref.} = \frac{P_{B-R_l,ref.}}{V_{B-R_l}} = \frac{P_{load,ref.} - P_{R,loss}}{V_{B-R_l}} \quad (7)$$

Note that for buck mode, the power on the low-voltage side is less than that needed at the load input terminals; therefore, the expected power loss must be subtracted from the load input power reference. For the boost mode, on the contrary, the power on the low-voltage side should be greater than that at the input terminals. However, the power at the input

terminals is negative, and the absolute value of the power on the low-voltage side should be greater than that required at the load terminals. Thus, equation (7) will work for both modes.

The current feedback from the low-voltage side (the current flowing into battery-R_l combination) is compared with the current reference derived in (7) to obtain an error signal that will be amplified and triangulated to make the switching signal for S_1 and S_2 in the buck and boost modes of operation, respectively.

As shown in Fig. 9, the control circuit of the controllable DC load consists of two similar control loops, each responsible for one mode of operation. The output of the buck control loop goes to S_1, while the output of the boost control loop goes to S_2. When the power reference signal is positive, buck mode has to be used, while boost mode must be used when the power reference signal is negative. The mode identification signal is sent to a pair of AND gates where this signal is ANDed with the output of each control loop. The signal leading to the AND gate of the boost control loop is inverted with a NOT gate. Thus, when the mode signal is high, the AND gate for the boost control loop will output a low signal to S_2, thus turning the switch off. When the mode signal is low, the AND gate for the buck control outputs a low signal to S_1, thus turning the switch off. Note that since the voltage polarities in the power circuit do not change as the mode of operation changes, power reversal is performed by reversing the direction of current. A negation block is used in the boost control loop to compensate for the fact that both reference and actual values for the current in boost mode are negative.

To control the switch S_3, it must be determined when the incoming power should go to the battery and when to the load resistor R_l. Obviously, if the converter is in boost mode, the load resistor must be disconnected. When the converter is in buck mode, the battery-resistor combination must absorb the power based on the following logic. If the battery charge is below the SOC limit, the incoming power should go to the battery; thus, the resistor should be disconnected. If the battery is charged up to the SOC limit, then the resistor should consume the whole incoming power. To realize this logic, the state-of-charge (SOC) of the battery is compared with a set value. In this study, the SOC limit of 96% was chosen to prevent the battery from overcharging. Assuming the converter is in buck mode, if the SOC is greater than 96%, the switch S_3 is turned on. When this switch is on, the resistor will draw 50A. However, if the load is not operating at maximum power, the incoming current to the B-R_l combination will be less than 50A. The remaining current should come from the battery, forcing the battery to discharge. When the battery discharges below 96% SOC, the switch is turned off. Then, the incoming current will charge the battery back to 96%, causing the switch to turn on again. This cycle will repeat itself until a braking sequence occurs. In order to reduce the potentially high switching frequency that results from this operation, a hysteresis controller can be implemented to make the switch S_3 turn on only if SOC exceeds 96% + ΔSOC and turn off when SOC falls below 96% - ΔSOC. When the drive cycle calls for a braking sequence, the converter will go into boost mode, the battery discharges and supplies power to the load terminals.

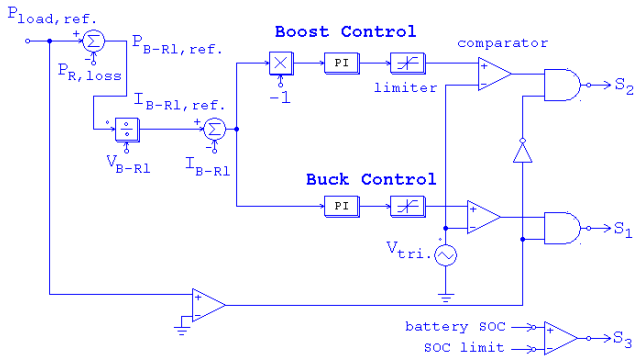

Fig. 9 Block diagram of control circuit of bidirectional controllable DC load

IV. Simulation Results

The regenerative controllable DC load was simulated using PSIM simulation package. In the simulation, only a small portion of the drive cycle shown in Fig. 8 was used to reduce the simulation run time. This portion is shown in Fig. 10. As stated before, the load was designed for a small-scale laboratory set-up; therefore, the power request of the full-size vehicle was scaled down 10 times so that it could be realized by the 3-kW controllable load. The controller uses a limiter is to keep the scaled power reference in the range [-3, 3] kW.

The PSIM simulation results for the power reference and the actual power at the load input terminals are shown in Fig. 11. The results verify excellent reference tracking of the load.

Fig. 10 Selected portion of the drive cycle of Fig. 8 and the corresponding power used for simulations

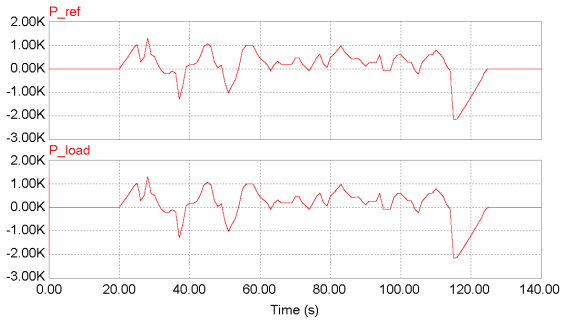

Fig. 11 Simulation Results: power reference (top) and actual power (bottom)

Fig. 12 shows the power at the input terminals of the load, the SOC of the battery, and the waveforms of the currents

through the battery and load resistor R_l. The initial value for SOC (95.5%) and the SOC limit (96%) have been intentionally chosen in such a way that the SOC limit is reached during buck mode of operation. As seen, when SOC hits the limit, the switch S_3 turns on to prevent battery from overcharging. The load resistor R_l will draw 50A, part of which will be supplied by the battery. When the battery SOC falls below the limit, S_3 turns off, letting battery SOC rise again. This high-frequency operation continues till the direction of power is reversed and the battery is discharged turning switch S_3 off for the rest of the regenerative braking (boost mode) period. Note that using a hysteresis controller can reduce the frequency of switching of S_3. Also, by setting the SOC limit to the right value, based on the prior knowledge of drive cycle and the corresponding power profile, it is likely to operate the load without any need for switching the load resistor R_l in and out by turning S_3 on and off. For example, for SOC limit of 96.5%, resistor R_l will never be switched in during the drive cycle simulated (Fig. 13). This would be the ideal condition; however, the resistor R_l is included in the power circuit for battery protection.

V. Conclusions

In this paper, a regenerative controllable DC load was designed based on the bidirectional buck-boost DC/DC converter topology. The load is capable of emulating a vehicular load during acceleration, cruising, deceleration and stopping periods. As a result, the load can incorporated in an electric vehicle test station and programmed to act as a vehicular load according to a power reference derived from a selected drive cycle. The load structure and control are simple; the component count is low; the load is stand-alone, as the battery supplies power to the control and switch driver circuits; and the design is scalable. The capability of the load in accurate tracking of the power reference has been verified through simulation results.

Appendix

The parameters used for calculating vehicle's required power are: Air density (ρ) = 1.2 kg/m^3, Drag coefficient (C) = 0.31, Vehicle's cross-sectional area (A) = 2.52 m^2, Vehicle's mass (m) = 1,227 kg, Gravitational acceleration (g) = 9.81 N/kg, Friction coefficient (μ) = 0.009.

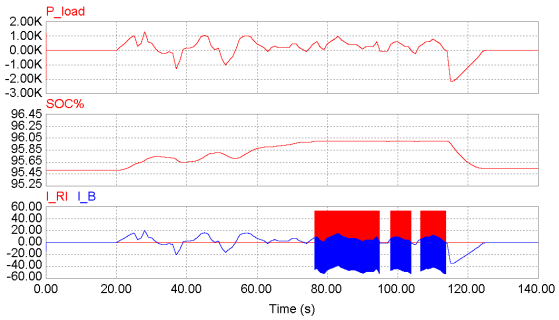

Fig. 12 Simulation Results for SOC limit of 96%: actual load (top), SOC% (middle) and currents through the battery and load resistor R_l (bottom)

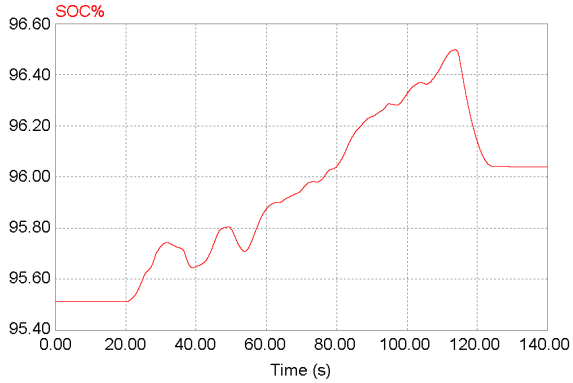

Fig. 13 Simulation Results for SOC limit of 96.5%: SOC%

References

[1] F. Wicks and K. Donnelly, "Modeling Regenerative Braking and Storage for Vehicles", *Proceedings of the 32nd Intersociety of the Energy Conversion Engineering Conference*, 1997, Vol. 3, pp. 2030-2035.

[2] Z. Chuanwei, B. Zhifeng, C. Binggang and L. Jingcheng, "Study on Regenerative Braking of Electric Vehicle", *Proceedings of the 4th International Power Electronics and Motion Control Conference*, 2004, Vol. 2, pp. 836-839.

[3] M. Kazerani, "A High-Performance Controllable DC Load", *Proceedings of 2007 IEEE International Symposium on Industrial Electronics* (*ISIE'07*), Vigo, Spain, June 4-7, 2007.

[4] K. Jin, X. Ruan, M. Yang and M. Xu, "A Novel Hybrid Fuel Cell Power System", *Proceedings of IEEE 2006 Power Electronics Specialists Conference* (*PESC '06*), 18-22 June 2006, pp. 1 – 7.

[5] S. Jang, T. Lee, W. Lee and C. Won, "Bi-directional DC-DC Converter for Fuel Cell Generation System", *Proceedings of 2004 IEEE Power Electronics Specialists Conference* (*PESC'04)*, Vol. 6, 20-25 June 2004, pp. 4722 – 4728.

[6] S. Inoue and H. Akagi, "A Bidirectional DC-DC Converter for an Energy Storage System with Galvanic Isolation", *IEEE Transactions on Power Electronics*, 2007, Vol. 22, No. 6, pp. 2299-2306.

[7] N. Mohan, T. Undeland and W. Robbins, Power Electronics: Converters, Applications and Design, 3rd Edition, John Wiley & Sons, Inc., 2003.

[8] J. Marshall and M. Kazerani, "Design of an Efficient Fuel Cell Vehicle Drivetrain, Featuring a Novel Boost Converter", Proceedings of 2005 IEEE Industrial Electronics Conference (IECON'05), 6-10 Nov. 2005, pp. 1229-1234.

[9] EnerSys, "Genesis Purelead XE and EP, Application Manual, 7th edition", http://www.enersys.com, accessed Feb. 5, 2009.

[10] Environmental Protection Agency, "Federal Test Procedure Revisions", http://www.epa.gov/otaq/sftp.htm#cycles, accessed Feb. 4, 2009.

[11] D. Halliday, R. Resnick and J. Walker, *Fundamentals of Physics*, 7th Edition, 2005, John Wiley and Sons, Inc.